

# **Central Lancashire Online Knowledge (CLoK)**

Title	Thermoreversible gelation in poly(ethylene oxide)/carbon black hybrid
	melts
Type	Article
URL	https://clok.uclan.ac.uk/id/eprint/11340/
DOI	https://doi.org/10.1016/j.polymer.2014.10.023
Date	2014
Citation	Kelarakis, Antonios, Krysmann, Marta and Giannelis, Emmanuel (2014)
	Thermoreversible gelation in poly(ethylene oxide)/carbon black hybrid
	melts. Polymer, 55 (24). pp. 6278-6281. ISSN 0032-3861
Creators	Kelarakis, Antonios, Krysmann, Marta and Giannelis, Emmanuel

It is advisable to refer to the publisher's version if you intend to cite from the work. https://doi.org/10.1016/j.polymer.2014.10.023

For information about Research at UCLan please go to <a href="http://www.uclan.ac.uk/research/">http://www.uclan.ac.uk/research/</a>

All outputs in CLoK are protected by Intellectual Property Rights law, including Copyright law. Copyright, IPR and Moral Rights for the works on this site are retained by the individual authors and/or other copyright owners. Terms and conditions for use of this material are defined in the <a href="http://clok.uclan.ac.uk/policies/">http://clok.uclan.ac.uk/policies/</a>

# Thermoreversible gelation in poly(ethylene oxide)/carbon black hybrid melts

# Antonios Kelarakis<sup>1</sup>, Marta J. Krysmann<sup>2</sup>, Emmanuel P. Giannelis<sup>3</sup>

1. Centre for Materials Science, School of Forensic and Investigative Sciences, University of Central Lancashire, Preston PR12HE, U.K.

akelarakis@uclan.ac.uk tel.004417724172

- 2. School of Pharmacy and Biomedical Sciences, University of Central Lancashire, Preston PR12HE, U.K.
- 3. Department of Materials Science and Engineering, Cornell University, Ithaca, NY 14853, USA

**Abstract** 

The study focuses on the structure and viscoelasticity of poly(ethylene oxide)/carbon black

fluids. The hybrids when subjected to extreme thermal annealing (at temperatures far above the

melting point of the matrix) exhibit a 3-4 orders of magnitude increase in viscosity. Surprisingly,

the effect is reversible and the viscosity reverts back to its initial value upon subsequent cooling.

This rather unique sol-gel transition in terms of strength, steepness and thermal reversibility

points to major structural rearrangements via extensive particle clustering, in agreement with

microscopy observations. In related systems it was found that when matrix-particle electrostatic

interactions are present the gelation is essentially diminished.

**Keywords:** poly(ethylene oxide), carbon black, gelation

2

### 1. Introduction

The evolution of physical gelation in colloidal fluids has been explained in terms of phase separation, connectivity percolation, jamming, kinetic and dynamic arrest (1). Although, the effect is frequently encountered in nature, a consensus for the underlying mechanism and a universal phase diagram have yet to emerge (2). It is nevertheless clear that under transient conditions gelation critically depends upon the dispersion state and the volume fraction of the suspended particles as well as the strength of short range attractions such as depletion, van der Waals and hydrophobic forces.

Typically, the occurrence of physical gelation in moderately or highly filled polymers is attributed to the built up of a network of nanoparticles that span large sections of the host (3). The sol-gel transition reflects the balance of the polymer-polymer, polymer-particle and particle-particle interactions and proceeds through direct particle aggregation or polymer mediated networking (4,5). Each one of those distinct contributions is thermodynamic in nature so that the flow properties of filled systems might follow a complex temperature- dependent profile.

In this work we report on an extreme case of thermoreversible gelation in poly(ethylene oxide) (PEO) melts reinforced with carbon black (CB). In particular, we demonstrate that aggressive thermal annealing at temperatures far above the melting point of the matrix ( $T_m$ = 65°C) leads to a 3-4 orders of magnitude enhancement in viscosity, and this behaviour is fully reversed upon subsequent cooling. We correlate the rheological effect in terms of strength, steepness and thermal reversibility to major structural rearrangements supported by microscopy studies.

From a fundamental perspective CB dispersions can be viewed as model fluids to gain insights on the local dynamics and the gelation mechanism in systems with short range attractions (6). From a technological viewpoint, the rheological behaviour of CB dispersions is directly related to the processability and performance of a series of materials such as paints, inks, batteries, tires, sensors, vapour detectors, and antistatic materials (7-9). Understanding and, ultimately, controlling the rheological behavior of those systems across a wide temperature range is essential for certain applications and the present study provides insights towards that direction. In addition, CB close mimic the structure and properties of soot particles that are spontaneously

released in the engine oil as a by-product of combustion and, to make things worse, they aggregate upon heating, further compromising the lubrication efficacy (10).

# 2. Experimental Section

 $\alpha$ -ω hydroxyl-terminated poly(ethylene oxide) (referred here as PEO) with weight average molecular weight MW=  $8x10^3$  g/mol was purchased from Polysciences Inc.  $\omega$  amine terminated ethylene oxide (EO)/propylene oxide (PO) copolymer with a molar ratio PO/EO=8/58 (trade name Surfonamine L300) was purchased from Huntsman and is referred here as PEO-NH<sub>2</sub>. Carbon black (CB) samples with -NH<sub>2</sub> or -SO<sub>3</sub> surface groups were obtained from Cabot and are referred to as CB-NH<sub>2</sub> and CB-SO<sub>3</sub>, respectively. Pristine montmorillonite (MMT-Na<sup>+</sup>) was provided by Southern Clay Products. Ludox silica (HS 30) was freeze-dried before use. All hybrids contained 5 wt.% particles and were prepared in an identical manner by melt mixing at  $90\,^{\circ}$ C for 4 h.

Rheological properties were determined using a Paar Physica Modular Compact Rheometer 300 (MCR 300) equipped with parallel plate geometry (diameter 25 mm). Measurements were performed in small amplitude oscillatory shear in a nitrogen atmosphere to suppress oxidative degradation. The frequency scans typically covered a range of angular frequency ( $\omega$ ) from 0.1 to 100 rad s<sup>-1</sup>. All temperature sweeps were recorded at a rate of 1 °C/min at  $\omega$ =10 rad s<sup>-1</sup>. Before any measurement the samples were kept for 160 °C for 30 min in the rheometer for thermal equilibration and structural relaxation.

Transmission Electron Microscopy (TEM) images were obtained using an A FEI T12 Spirit operated at 120 kV. A droplet of a sample (0.05 mg/mL in ethanol) was deposited on a carbon coated cupper grid (Agar Scientific, USA) and dried in air. The grids were subjected to thermal annealing in inert atmosphere at 160 °C for 30 min. Subsequently, the grids were quenched in liquid nitrogen (and removed from liquid nitrogen just before the TEM imaging) or allowed to cool slowly at a room temperature.

#### 3. Results and Discussion

Figure 1 compares the complex viscosity ( $\eta^*$ ) of a series of PEO hybrid melts with the corresponding neat matrix. Isochronal cooling scans were performed on all samples that were thermally annealed at 160 °C for 30 min. As expected the neat polymer shows positive flow activation energy within the entire temperature range considered with  $\eta^*$  monotonically increasing upon cooling. In contrast, all three hybrid melts based on clay, silica and CB-SO<sub>3</sub> respectively, show first a decrease of  $\eta^*$  upon cooling followed by the expected increase. In other words, all hybrids show a minimum at an intermediate temperature (in the range 110-130 °C). We recently reported the anomalous behaviour for the PEO/clay system and have included it in this study for comparison with the far more dramatic case of the PEO/ CB-SO<sub>3</sub> hybrid. We attributed the anomalous rheological behaviour of the former to rearrangements of the polymer chains and/ or the clay platelets in the melt (11).

In general, time and temperature dependent morphologies in filled systems are attributed to the slow diffusion of the embedded particles within the viscous matrix, in a manner that either leads towards improved dispersion or to particle clustering. For example, in poly(methyl acrylate)/silica nanocomposites SAXS data and TEM imaging indicate that particle dispersion is improved following extended thermal treatment (12). In contrast, in PEO/silica nanocomposites, AFM studies reveal the partial flocculation of the filler as a result of thermal annealing (13). The high-temperature viscosity upturn reported for our PEO/silica system (Figure 1) is in line with this observation. Likewise, TEM images indicate that thermal annealing promotes CB clustering in a polystyrene matrix (14).

In the PEO/CB-SO<sub>3</sub> hybrids,  $\eta^*$  is close to 8800 Pa s at 160 °C, displays a minimum of 4 Pa s at 110 °C and becomes 8 Pa s at 75 °C. The isothermal frequency scans shown in Figure 2 further support the dramatic nature of the sol-gel transition. At 160 °C the melt exhibits solid-like response with G'> G" within the entire frequency window considered, while G' does not vary with frequency (G' and G" stand for storage and loss modulus, respectively). However, the same sample at 75 °C shows a characteristic liquid-like behaviour with G' <G" within the entire frequency window. The rheological data at 160 °C suggest a much more robust network compared to that typically seen in composite materials where the deviations from the ideal melt behaviour are limited only to the low frequency range (15).

Although there is some hysteresis for cooling and heating (Figure 3), it is clear that the thermal treatment does not result in permanent structural reorganization in the PEO/CB-NH<sub>2</sub> melt. Despite its dramatic nature, the sol-gel transition is fully thermoreversible and highly reproducible. This aspect of the rheological behaviour is unique for the present system and is further explored and discussed below.

TEM images of the PEO/CB-SO<sub>3</sub> hybrid that has been subjected to extensive thermal annealing at 160 °C for 30 min (under inert atmosphere) are shown in Figure 4. The system was cooled down slowly in order to reach structural and thermal relaxation. The TEM images reveal the presence of CB aggregates composed of primary particles with a diameter close to 30 nm. The images indicate good wetting of the aggregates and a polymer layer around the CB particles can be discerned.

Figure 5 shows TEM images of the PEO/CB-SO<sub>3</sub> hybrid that has experienced similar thermal annealing, but it was then quench-cooled in liquid nitrogen. The idea behind this treatment is that a rapidly frozen sample should preserve to a certain extent the structural information of the melt. Clearly, in the quench-cooled hybrid larger particle clusters are present, while the polymeric shell around the carbon particles appears to be thinner. All in all, the TEM images suggest that the morphological characteristics of the hybrids largely vary upon the cooling conditions.

To gain further insights on the gelation mechanism we investigated a series of CB hybrids based on the amine-terminated copolymer PEO-NH<sub>2</sub> (see experimental section for details). The rheological plots shown in Figure 6 indicate that only the melt filled with CB-NH<sub>2</sub> show a considerable high temperature viscosity enhancement, while the melt filled with CB-SO<sub>3</sub> does not show this trend. We believe that the favourable interactions between the amine groups of the matrix and the acidic groups in the surface of CB-SO<sub>3</sub> stabilise the dispersions and inhibit the formation of larger aggregates at high temperatures. Similar types of electrostatic interactions have been employed to develop self-suspended nanoparticles with remarkable stability and uniformity (16). We note that controlling or diminishing the high temperature rheological

enhancements in CB based materials is essential for certain applications such as printing inks, lubricants, etc. and the present study suggests effective pathways towards this goal.

The structure development in thermally annealed CB melts and dispersions has been the subject of several reports. To that end, the evolution of a percolated network in polystyrene/CB (17) and polyethylene/CB (18) melts was monitored by simultaneous measurements of electrical resistance and G' as a function of filler volume fraction, annealing time and temperature. In those systems the annealing induced networking has been modelled as a first order kinetics aggregation process due to the diffusion of small isolated aggregates towards a pre-existing CB backbone. In another study, CB suspensions in a hydrocarbon fluid (stabilized with adsorbed polyisobutylene succinimide dispersant) were shown to exhibit significant changes in rheology upon heating (19). It was concluded that the collapse of the dispersant chain at high temperature promotes the formation of strongly aggregated clusters that are directly observable under an optical microscope (19).

Despite significant interest on the sol-gel transition in CB based materials, little is known about the reversibility or not of the effect and particle clustering is generally considered to be permanent. Nevertheless, it is clear that percolated CB networks are prone to mechanical deformations and even small shear forces can destroy the 3-D connectivity in CB/ polypropylene carbonate suspensions causing a steep drop in viscosity and conductivity (20). In CB/varnish dispersions, the viscosity increases with heating due to the formation of CB clusters that remain intact during subsequent cooling, but do not sustain shearing (21). In addition, in concentrated CB aqueous suspensions stabilised by PEO copolymers the viscosity increases above the critical flocculation temperature, but the effect is thermoreversible and the suspension restores back its initial flow properties upon cooling (22).

With respect to other related systems, we note that deformation events destruct the CNT network in a polycarbonate melt, but the 3-D connectivity of the aggregates is restored after a certain recovery period (23). Moreover, the viscosity of CNT/oil dispersions increases at moderate temperatures due to particle agglomeration, but then decreases upon further heating (24). In another study it has been demonstrated that the physical gelation in an ethylene–propylene random copolymer induced by carbon nanofibers is thermo-reversible (3).

Returning to the underlying mechanism in our system, we note that physical gelation reflects the interplay between polymer adsorption to the filler surface and the tendency of CB particles for clustering. When polymer is adsorbed to solid substrates, the inner polymer layer is permanently attached to the substrate and resists detachment even under intensive chemical leaching, but the outer polymer layer is only loosely attached and displays contraction upon heating, in a thermoreversible manner (25,26). The combination of those factors might account for the behaviour observed here, e.g. tightly attached polymer shell does not allow irreversible aggregation of CB, and as the polymer layer expands at lower temperature the connectivity of the CB aggregates is lost. However, when strong electrostatic host-guest interactions are present the tendency for CB agglomeration is suppressed.

#### 4. Conclusion

We demonstrate a unique case of thermoreversible physical gelation in PEO/CB melts. At temperatures far above the melting point of the matrix, pronounced particle clustering gives rise to dramatic rheological enhancements indicative of a sol-gel transition. In contrast to the expected trend for irreversible aggregation, the viscosity of PEO/CB melts reverts back to its initial value after a complete heating-cooling cycle. At the same time, in selected systems strong host-guest interactions inhibit CB clustering so that viscoelastic enhancements do not take place upon heating.

# Acknowledgements

This material is partially based on work supported as part of the Energy Materials Center at Cornell, an Energy Frontier Research Center funded by the U.S. Department of Energy, Office of Science, Office of Basic Energy Sciences under Award Number DE-SC0001086. This publication is based on work supported in part by Award No. KUS-C1-018-02, made by King Abdullah University of Science and Technology (KAUST).

### References

- 1. Lu PJ, Zaccarelli E, Ciulla F, Schofield AB, Sciortino F, Weitz DA. Nature 2008; 453: 499
- 2. Zaccarelli E. J. Phys.: Condens. Matter. 2007; 19:323101
- 3. Kelarakis A, Yoon K, Somani RH, Chen X, Hsiao BS, Chu B. Polymer 2005;46:11591-11599
- 4. Surve M, Pryamitsyn V, Canesan V. Physical Review Letters 2006; 96:177805
- 5. Zhu Z, Thompson T, Wang SQ, von Meerwall ED, Halasa A. Macromolecules 2005;38: 8816-8824
- 6. Trappe V, Weitz DA. Phys. Rev. Lett. 2000; 85: 449-452
- 7. "Carbon Black: Science and Technology" Marcel Dekker, Inc. (New York) 1993 ed. by Donnet JB, Bansal RC, Wang MJ.
- 8. Dominko R, Gaberscek M, Drofenik J, Bele M, Pejovnik S, Jamnik J. J. Power Sources 2003;119: 770-773
- 9. Lonergan MC, Severin EJ, Doleman BJ, Beader SA, Grubbs RH, Lewis NS. Chem. Mater. 1996; 8: 2298–2312
- 10. Clague ADH, Donnet JB, Wang TK, Peng JCM. Carbon 1999; 37: 1553-1565
- 11. Kelarakis A, Giannelis EP. Polymer 2011;52: 2221-2227
- 12. Janes DW, Moll JF, Harton SE, Durning CJ. Macromolecules 2011;44:4920-4927
- 13. Zhiang Q, Archer LA. Langmuir 2002;18:10435-10442
- 14. Tan Y, Yin X, Chen M, Song, Y, Zheng Q. J. Rheol. 2011;55:965-979
- 15. Kelarakis A, Hayrapetyan S, Ansari S, Fang J, Estevez L, Giannelis EP. Polymer 2010; 51, 469-474
- 16. Rodriguez R, Herrera R, Archer LA, Giannelis EP. Advanced Materials 2008;20: 4353-4358
- 17. Cao Q, Song Y, Tan Y, Zheng Q. Carbon 2010;48: 4268-4275

- 18. Cao Q, Song Y, Tan Y, Zheng Q. Polymer 2009;50: 6350-6356
- 19. Won YY, Meeker SP, Trappe V, Weitz DA, Diggs NZ, Emert JI. Langmuir 2005;21:924-932
- 20. Youssry M, Madec L, Soudan P, Cerbelaud M, Guyomard D, Lestriez B. Phys. Chem. Chem Phys. 2013;15:14476-11486
- 21. Aoki Y. Rheol. Acta. 2011;50: 787-793
- 22. Miano F, Bailey A, Luckham PF, Tandros TF. Colloids and Surfaces 1992;62:111-118
- 23. Alig I, Skipa T, Lellinger D, Potschke P. Polymer 2008; 49: 3524–3532
- 24. Yang Y, Grulke EA, Zhang ZG, Wu G. Colloids and Surfaces A: Physicochem, Eng, Aspects 2007;298: 216-224
- 25. Orts WJ, van Zanten JH, Wu W, Satija SK. Physical Review Letters 71; 1993:867-870
- 26. Jiang N, Sang J, Di X, Endoh MK, Kanga T. Macromolecules 2014;47:2682-2689

# **Figures**

- **Figure 1**. Temperature dependence of complex viscosity ( $\eta^*$ ) of PEO hybrid melts during isochronal cooling ramps ( $\omega$ =10 rad s<sup>-1</sup>, cooling rate 1 °C/min). Green triangles, red squares, blue diamonds refer to silica, CB-SO<sub>3</sub> and clay filled melts, respectively. For comparison, the neat polymer melt is also shown (black circles).
- **Figure 2.** Frequency dependence of the storage (filled symbols) and loss (open symbols) modulus for PEO/ CB-SO<sub>3</sub> hybrids at 75 °C (circles) and 160 °C (squares).
- **Figure 3**. Temperature dependence of complex viscosity ( $\eta^*$ ) of PEO/CB-NH<sub>2</sub> hybrid melts during isochronal cooling (red squares) and subsequent heating ramp (blue triangles) ( $\omega$ =10 rad s<sup>-1</sup>, cooling/heating rate 1 °C/min).
- **Figure 4.** TEM images of the slowly-cooled PEO/CB-SO<sub>3</sub> hybrid following thermal annealing at 160 °C.
- **Figure 5**. TEM images of the quench-cooled PEO/CB-SO<sub>3</sub> hybrid following thermal annealing at 160 °C.
- **Figure 6**. Temperature dependence of complex viscosity ( $\eta^*$ ) of PEO/CB-NH<sub>2</sub> (red squares) and PEO/CB-SO<sub>3</sub> (blue triangles) hybrid melts during isochronal cooling ramps ( $\omega$ =10 rad s<sup>-1</sup>, cooling rate 1 °C/min). For comparison, the neat polymer melt (black circles) is also shown.

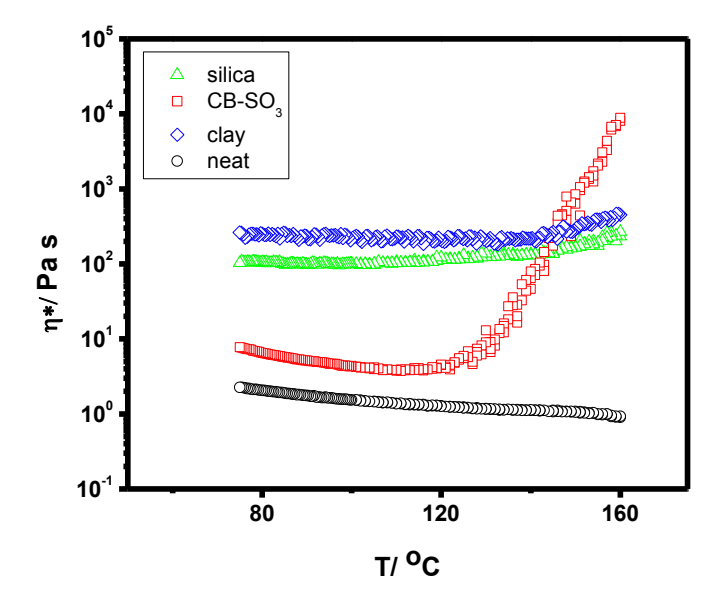


Figure 1.

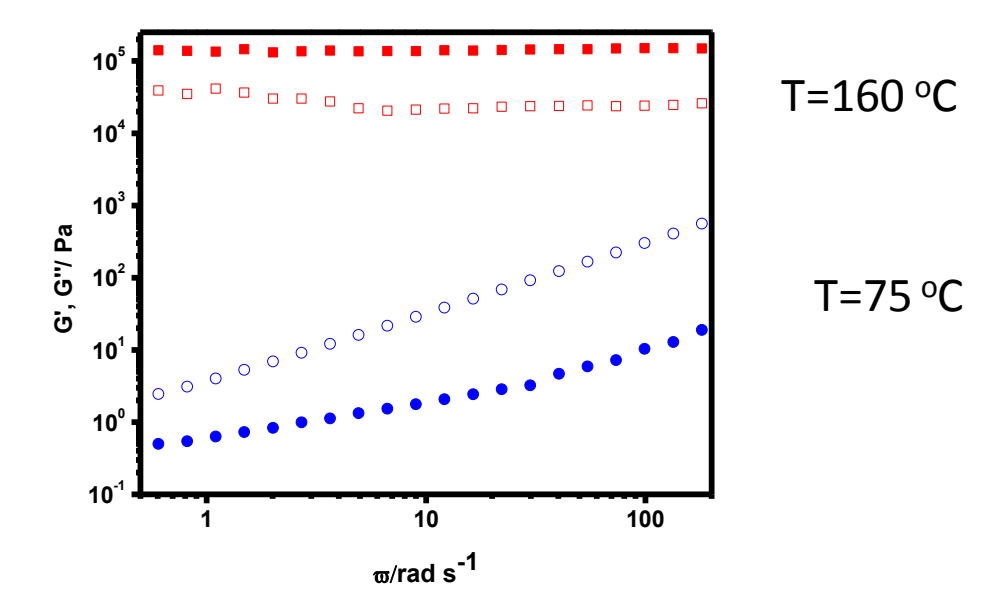


Figure 2.

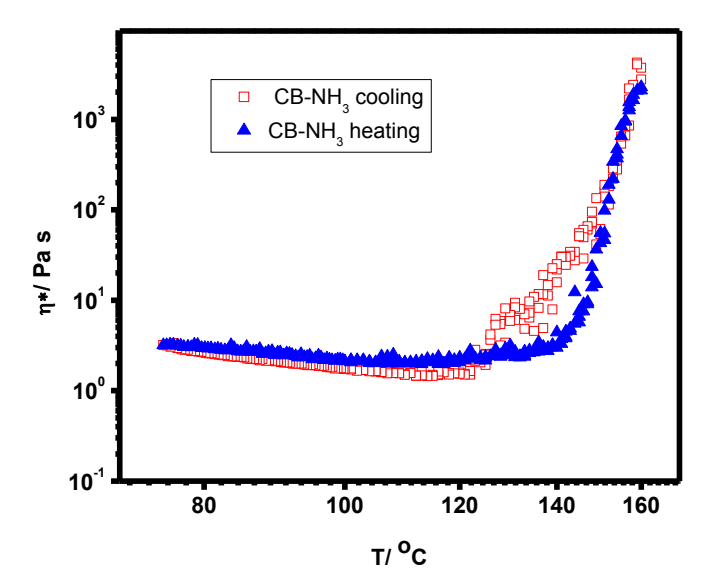
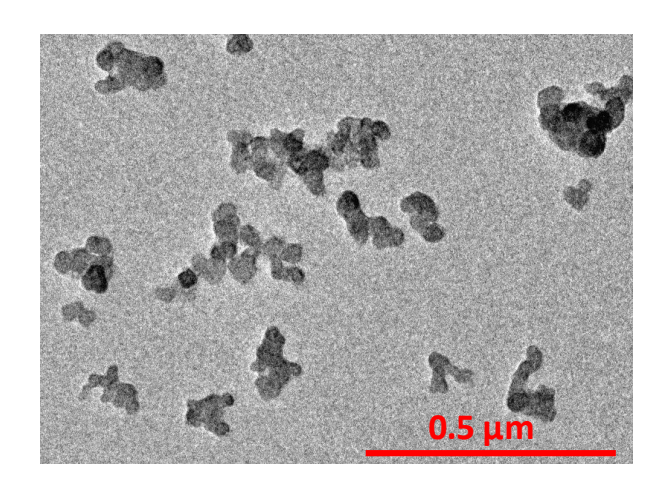


Figure 3.



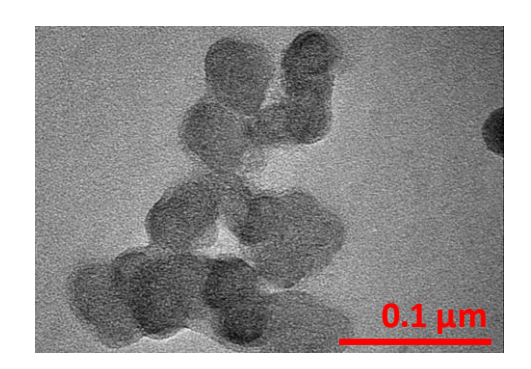
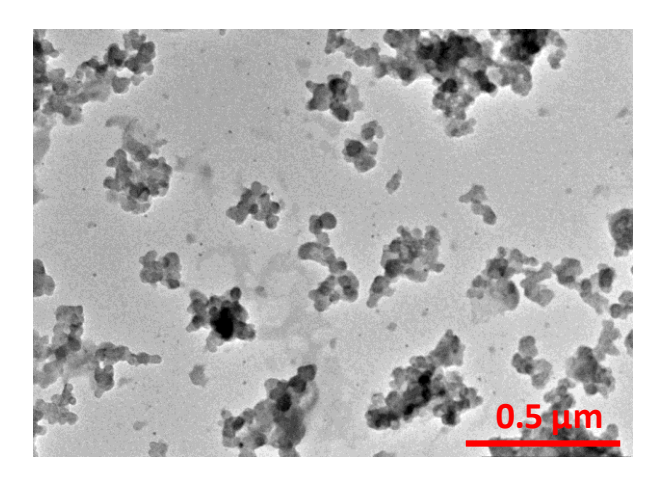


Figure 4.



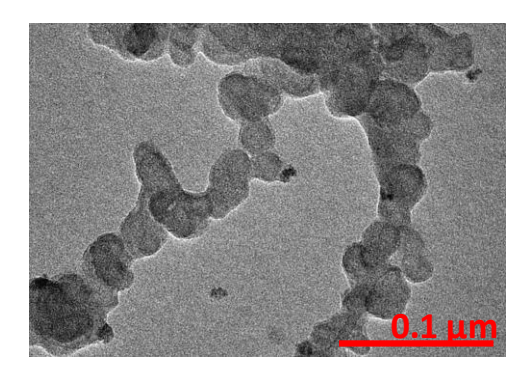


Figure 5.

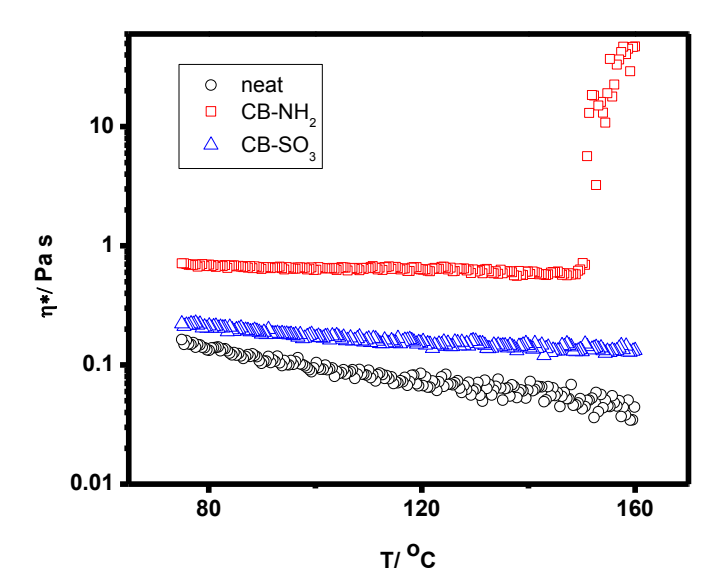


Figure 6.